JCI The Journal of Clinical Investigation

Bacterial exploitation of phosphorylcholine mimicry suppresses inflammation to promote airway infection

Christopher B. Hergott, Aoife M. Roche, Nikhil A. Naidu, Clementina Mesaros, Ian A. Blair, Jeffrey N. Weiser

J Clin Invest. 2015;125(10):3878-3890. https://doi.org/10.1172/JCI81888.

Research Article **Pulmonology**

Regulation of neutrophil activity is critical for immune evasion among extracellular pathogens, yet the mechanisms by which many bacteria disrupt phagocyte function remain unclear. Here, we have shown that the respiratory pathogen *Streptococcus pneumoniae* disables neutrophils by exploiting molecular mimicry to degrade platelet-activating factor (PAF), a host-derived inflammatory phospholipid. Using mass spectrometry and murine upper airway infection models, we demonstrated that phosphorylcholine (ChoP) moieties that are shared by PAF and the bacterial cell wall allow *S. pneumoniae* to leverage a ChoP-remodeling enzyme (Pce) to remove PAF from the airway.*S. pneumoniae*–mediated PAF deprivation impaired viability, activation, and bactericidal capacity among responding neutrophils. In the absence of Pce, neutrophils rapidly cleared *S. pneumoniae* from the airway and impeded invasive disease and transmission between mice. Abrogation of PAF signaling rendered Pce dispensable for *S. pneumoniae* persistence, reinforcing that this enzyme deprives neutrophils of essential PAF-mediated stimulation. Accordingly, exogenous activation of neutrophils overwhelmed Pce-mediated phagocyte disruption. *Haemophilus influenzae* also uses an enzyme, GlpQ, to hydrolyze ChoP and subvert PAF function, suggesting that mimicry-driven immune evasion is a common paradigm among respiratory pathogens. These results identify a mechanism by which shared molecular structures enable microbial enzymes to subvert host lipid signaling, suppress inflammation, and ensure bacterial persistence at the mucosa.

Bacterial exploitation of phosphorylcholine mimicry suppresses inflammation to promote airway infection

Christopher B. Hergott,[1] Aoife M. Roche,[1] Nikhil A. Naidu,[1] Clementina Mesaros,[2] Ian A. Blair,[2] and Jeffrey N. Weiser[1,3,4]

[1]Department of Microbiology, [2]Department of Systems Pharmacology and Translational Therapeutics, and [3]Department of Pediatrics, Perelman School of Medicine, University of Pennsylvania, Philadelphia, Pennsylvania, USA. [4]Department of Microbiology, New York University School of Medicine, New York, New York, USA.

Regulation of neutrophil activity is critical for immune evasion among extracellular pathogens, yet the mechanisms by which many bacteria disrupt phagocyte function remain unclear. Here, we have shown that the respiratory pathogen *Streptococcus pneumoniae* disables neutrophils by exploiting molecular mimicry to degrade platelet-activating factor (PAF), a host-derived inflammatory phospholipid. Using mass spectrometry and murine upper airway infection models, we demonstrated that phosphorylcholine (ChoP) moieties that are shared by PAF and the bacterial cell wall allow *S. pneumoniae* to leverage a ChoP-remodeling enzyme (Pce) to remove PAF from the airway. *S. pneumoniae*–mediated PAF deprivation impaired viability, activation, and bactericidal capacity among responding neutrophils. In the absence of Pce, neutrophils rapidly cleared *S. pneumoniae* from the airway and impeded invasive disease and transmission between mice. Abrogation of PAF signaling rendered Pce dispensable for *S. pneumoniae* persistence, reinforcing that this enzyme deprives neutrophils of essential PAF-mediated stimulation. Accordingly, exogenous activation of neutrophils overwhelmed Pce-mediated phagocyte disruption. *Haemophilus influenzae* also uses an enzyme, GlpQ, to hydrolyze ChoP and subvert PAF function, suggesting that mimicry-driven immune evasion is a common paradigm among respiratory pathogens. These results identify a mechanism by which shared molecular structures enable microbial enzymes to subvert host lipid signaling, suppress inflammation, and ensure bacterial persistence at the mucosa.

Introduction

Neutrophils comprise an essential component of the acute inflammatory response to pathogens, particularly that against extracellular bacteria that reside on mucosal surfaces (1, 2). Typically first among leukocytes recruited to sites of infection, neutrophils exert potent bactericidal activity, impede microbial dissemination from epithelial barriers, and inhibit bacterial transmission between hosts (3–5). In turn, opportunistic microbes have evolved strategies to evade the neutrophils they elicit, the mechanisms of which have long been the subject of intensive study (6, 7). However, as the understanding of neutrophil biology has advanced, it has become clear that neutrophil bactericidal capacity is regulated dynamically and locally at inflamed sites (8) and that some pathogens directly manipulate the phagocyte activation state to inhibit microbial clearance at sites of infection (9, 10). Our understanding of the mechanisms by which neutrophil phagocytic function is suppressed in vivo remains incomplete.

Streptococcus pneumoniae, known as the pneumococcus, was among the first pathogens for which neutrophil evasion mechanisms were proposed (11–13). A leading cause of gram-positive bacterial pneumonia, sepsis, and meningitis, the pneumococcus causes nearly 1 million deaths each year worldwide and is estimated to be responsible for more than 100,000 hospitalizations in the United States annually (14, 15). All pneumococcal infections begin with asymptomatic colonization of the upper airway, and clinical studies have observed that progression from benign carriage to invasive infection often occurs only a few days after acquisition of upper airway infection (16–18). This coincides with the peak of neutrophil influx into the airway lumen and implies that pneumococcus-neutrophil interactions in the upper airway may govern the balance between bacterial clearance and disease (19, 20).

Pneumococcal resistance against neutrophils has traditionally been ascribed to its thick polysaccharide capsule, which serves to shield the bacterium from opsonization with complement or antibodies that would otherwise hasten phagocytic uptake (21, 22). However, in contrast to that in the lungs or bloodstream (23), pneumococcal resistance to neutrophils in the upper airway does not rely on antibody or complement evasion (24, 25). Further, colonizing pneumococci express markedly less capsular polysaccharide compared with blood and lung isolates, exposing cell wall components long known to be targets for immune recognition (26). Together, this suggests that capsule-mediated antiphagocytosis fails to fully explain pneumococcal neutrophil evasion in the upper airway. We sought to determine whether pneumococci instead disarm the phagocytic function of neutrophils recruited to the airway lumen, rendering them unable to mediate acute bacterial clearance.

Molecular mimicry is among the most widely conserved mechanisms by which bacteria evade immunity, exploiting the host's inability to recognize self-derived molecular structures (27). The pneumococcus, like many other airway bacteria, capitalizes on this vulnerability by displaying the host-derived small molecule phosphorylcholine (ChoP) on its surface. Decoration of pneumococcal cell wall components with ChoP is essential for bacterial fitness and is necessary to inhibit bacterial opsoniza-

Conflict of interest: The authors have declared that no conflict of interest exists.
Submitted: March 16, 2015; **Accepted:** July 23, 2015.
Reference information: *J Clin Invest*. 2015;125(10):3878–3890. doi:10.1172/JCI81888.

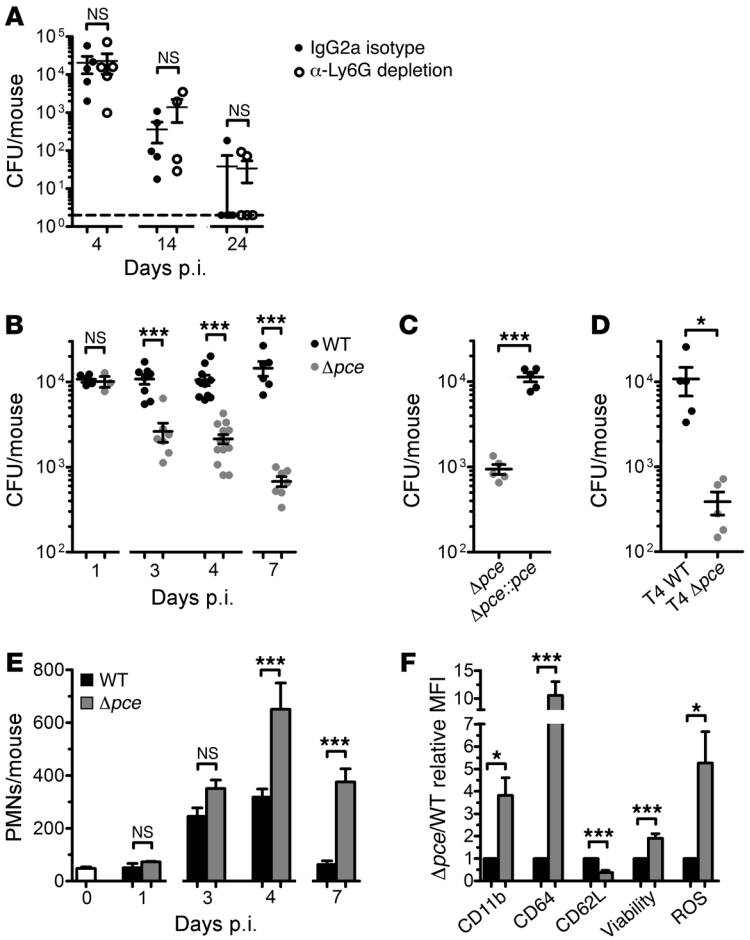

Figure 1. Pce-deficient pneumococci exhibit impaired persistence in the upper airway and elicit the recruitment of more activated, viable, and durable neutrophils to the nasal lumen. (**A**) Bacterial clearance in mice inoculated with WT pneumococci, strain P1121 (Type 23F), with (white circles) or without (black circles) systemic neutrophil depletion (n = 4–5 mice per condition, limit of detection [LOD] = 2). (**B**) Survival of WT P1121 (black) or P1121Δ*pce* (gray) pneumococci in the murine upper airway (n = 4–14). (**C**) Day-7 survival of P1121Δ*pce* mutant generated by in-frame, unmarked deletion (Δ*pce*) and with genetic correction (Δ*pce::pce*) (n = 5). (**D**) Day 7 survival of WT and Δ*pce* pneumococci on a type 4 (T4, TIGR4) pneumococcal genetic background (n = 5). (**E**) Quantification of neutrophils ($CD45^+CD11b^+Ly6G^+$) obtained from the upper airway lumen by nasal lavage before (n = 3) and after (n = 4–11) inoculation with WT (black) or Δ*pce* (gray) pneumococci. (**F**) Flow cytometric characterization of luminal neutrophils elicited by infection with WT or Δ*pce* pneumococci on day 4 p.i. (n = 6–8). Note that not all axes are continuous, and gaps in axes represent gaps in time. Dotted lines represent the LOD. Statistical significance was assessed by 1-way ANOVA with Newman-Keuls post test for comparisons of more than 2 conditions (**A**, **B**, and **E**), Student's t test for 2-group comparisons (**C** and **D**), and 1-sample Student's t test relative to null = 1 for relative MFI measurements (**F**). $^*P < 0.05$, $^{***}P < 0.001$.

tion (28). However, ChoP moieties are also found within a wide range of mammalian phospholipids, including those that function as secreted, proinflammatory lipid mediators (29). The receptor for one such host lipid, platelet-activating factor (PAF), has been shown to be a docking site for pneumococcal ChoP during epithelial cell adherence, highlighting that the PAF/PAFR axis may be a particularly important target for ChoP mimicry in the airway (30). PAF is secreted rapidly into the airway lumen in response to diverse inflammatory stimuli, including bacterial infection (31, 32). Though first identified as a mediator of systemic inflammation and platelet aggregation (33, 34), PAF was subsequently found to potently stimulate neutrophil phagocytic capacity and bactericidal function (35, 36). PAF binding to its G protein–coupled receptor on neutrophils triggers multiple intracellular signaling pathways (including PI3K, MAPK, PKA, PLC, and PLA2) to stimulate cellular viability, surface expression of bacterial uptake receptors, and mobilization of bactericidal machinery (37–40). Despite the central role PAF plays in regulating neutrophil function at mucosal surfaces, it remains unexplored whether ChoP mimicry can suppress PAF-mediated neutrophil activation.

Here, we used a murine upper airway infection model and primary human neutrophils to uncover an enzymatic mechanism by which molecular mimicry can be exploited by bacteria to modulate innate immunity. In a previously reported screen, we identified *pce,* encoding a cell wall–bound ChoP esterase (also known as CbpE), as a pneumococcal gene potentially contributing to evasion of neutrophil-mediated killing (41). We now demonstrate that *S. pneumoniae* uses Pce to hydrolyze ChoP from host-derived PAF in the lumen of the airway. The absence of functional PAF deprives infiltrating neutrophils of stimulatory signals necessary for optimal phagocyte activation and effective bacterial clearance, allowing pneumococci to persist in the airway, disseminate systemically, and transmit efficiently between hosts. We found that this exploitation of molecular mimicry is functionally conserved among multiple ChoP-bearing airway microbes, as the gram-negative pathogen *Haemophilus influenzae* uses a surface-bound phosphodiesterase, GlpQ, to hydrolyze ChoP and subvert PAF-mediated stimulation of acute inflammation.

Results

Neutrophils fail to contribute to mucosal defense during S. pneumoniae upper airway infection. We first sought to determine the contribution of acute inflammation to the control of pneumococcal upper airway infection. Mice treated every 4 days with either neutrophil-depleting (anti-Ly6G) (42) or IgG2a isotype control antibody were inoculated with a clinical isolate of *S. pneumoniae* (serotype 23F) and sacrificed at 4, 14, and 24 days post inoculation (p.i.). Neutrophil depletion was verified by flow cytometry (data not shown), and pneumococcal CFU from nasal lavages were enumerated at each time point. Consistent with previous observations during early infection (43), we found that neutropenic and control mice cleared pneumococci at equivalent rates over a 24-day period

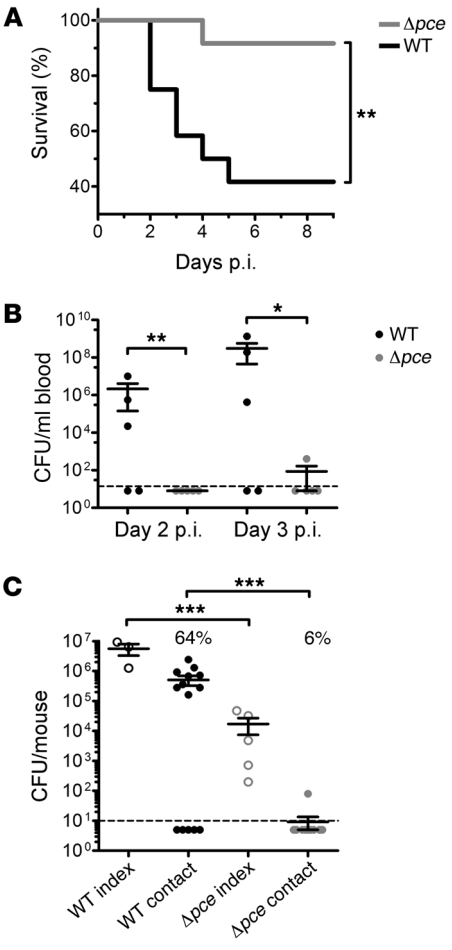

Figure 2. Pce promotes invasive pneumococcal disease and bacterial transmission between mice. (**A**) Survival of adult mice inoculated i.n. with WT (black) or Δ*pce* (gray) pneumococci of invasive strain P1547 (type 6A) (n = 12 mice per condition from 3 independent experiments). Statistical significance was assessed by the Mantel-Cox test. (**B**) Enumeration of CFU in the blood of mice infected with WT or Δ*pce* P1547 pneumococci as above (n = 5, LOD = 14). (**C**) Infant murine transmission. Upper airway lavage CFU enumerated from index (white circles, n = 3–4) and contact (black circles, n = 14–18) pups on day 14 of life and after index mice were inoculated with WT (black) or Δ*pce* (gray) pneumococci on day 4 of life. All pups were infected i.n. with influenza on day 8. Numerical values above contact mice columns represent the percentage of acquisition (LOD = 10). Transmission data reflect 3 independent experiments. In **B** and **C**, statistical significance was assessed by 1-way ANOVA with Newman-Keuls post test. *P < 0.05, **P < 0.01, ***P < 0.001.

(Figure 1A). These results suggested that, despite their rapid influx into the airway lumen following acquisition of infection (43), neutrophils failed to exert significant bactericidal pressure against *S. pneumoniae* in the upper airway.

Pneumococcal Pce esterase inhibits bacterial clearance and neutrophil activation. We next asked whether Pce esterase contributes to pneumococcal evasion of acute clearance from the airway. Mice inoculated with WT or Pce-deficient (Δ*pce*) pneumococci were sacrificed and lavaged for bacterial enumeration 1, 3, 4, and 7 days p.i., corresponding to the period during which neutrophilic inflammation is most prominent (20). While WT bacteria persisted at maximal density over the first week of infection, Δ*pce* pneumococci exhibited a survival defect that exceeded 20-fold by day 7 p.i. (Figure 1B). Notably, WT and Δ*pce* bacterial loads were equivalent at 1 day p.i., suggesting that differential inoculum retention or impaired establishment of infection was unlikely to explain the mutant's subsequent persistence defect. The poor survival of Δ*pce* pneumococci was recapitulated with an independently constructed unmarked, in-frame deletion mutant, restored upon genetic correction (Figure 1C) and preserved in a distinct serotype 4 isolate (Figure 1D). By day 14 p.i., Δ*pce* bacteria were effectively cleared, while WT pneumococci persisted at high levels (Supplemental Figure 1A; supplemental material available online with this article; doi:10.1172/JCI81888DS1). Collectively, these findings suggested that Pce is necessary for effective pneumococcal persistence during acute infection of the upper airway.

We then performed flow cytometry to characterize the acute inflammatory response to WT and Δ*pce* bacteria. Neutrophils dominated the cellular infiltrates elicited by both WT and Δ*pce* pneumococci (>95% of CD45$^+$ events, Supplemental Figure 1C). Despite lower bacterial density in the airway, mice inoculated with the Δ*pce* mutant exhibited elevations in the maximum density and, more markedly, the duration of neutrophil influx (Figure 1E). Congruent with bacterial load measurements, neutrophils persisted in the airway lumen through day 14 p.i. in Δ*pce*-infected mice but were nearly absent in response to WT pneumococci (Supplemental Figure 1B).

The more robust acute inflammatory response observed in the absence of Pce led us to hypothesize that the enzyme may perturb the qualitative capacity of neutrophils to persist and clear bacteria. Accordingly, we predicted that neutrophils recruited by Δ*pce* pneumococci would exhibit greater activation and superior phagocytic capabilities. To assess antimicrobial capacity in vivo, we functionally characterized the neutrophils responding to WT versus Δ*pce* bacteria by flow cytometry (Figure 1F). Compared with neutrophils elicited by WT pneumococci, those elicited by the mutant exhibited significantly elevated expression of CD11b (CR3) and CD64 (FcγRI) — which serve as both activation markers and bacterial uptake receptors (2, 39, 44) — and greater than 2-fold enhanced shedding of CD62L (L-selectin), a marker for inflammation-induced neutrophil activation (45, 46). Luminal neutrophils elicited by Δ*pce* bacteria included approximately twice as many viable cells compared with those responding to WT, a finding consistent with their enhanced persistence in the airway lumen. Last, Δ*pce*-elicited neutrophils exhibited an approximately 5-fold increase in ROS production per cell (as detected by CM-H_2DCFDA dye staining) over those recruited by WT bacteria, underscoring their enhanced bactericidal capacity (3). Together, these findings implied that Pce esterase impairs the cellular viability and phagocytic functionality of neutrophils upon their arrival in the airway lumen.

Pce promotes invasive pneumococcal disease and bacterial transmission between mice. A number of clinical and animal studies have found pneumococcal load in the upper airway to be strongly associated with both the onset and severity of subsequent invasive disease (16, 47) as well as the risk of pneumococcal transmission between hosts (5, 18). We asked whether the survival deficit exhibited by Δ*pce* pneumococci during infection of the upper airway corresponded with differences in these clinically important outcomes. To gauge relative invasive disease risk, we inoculated mice i.n. with

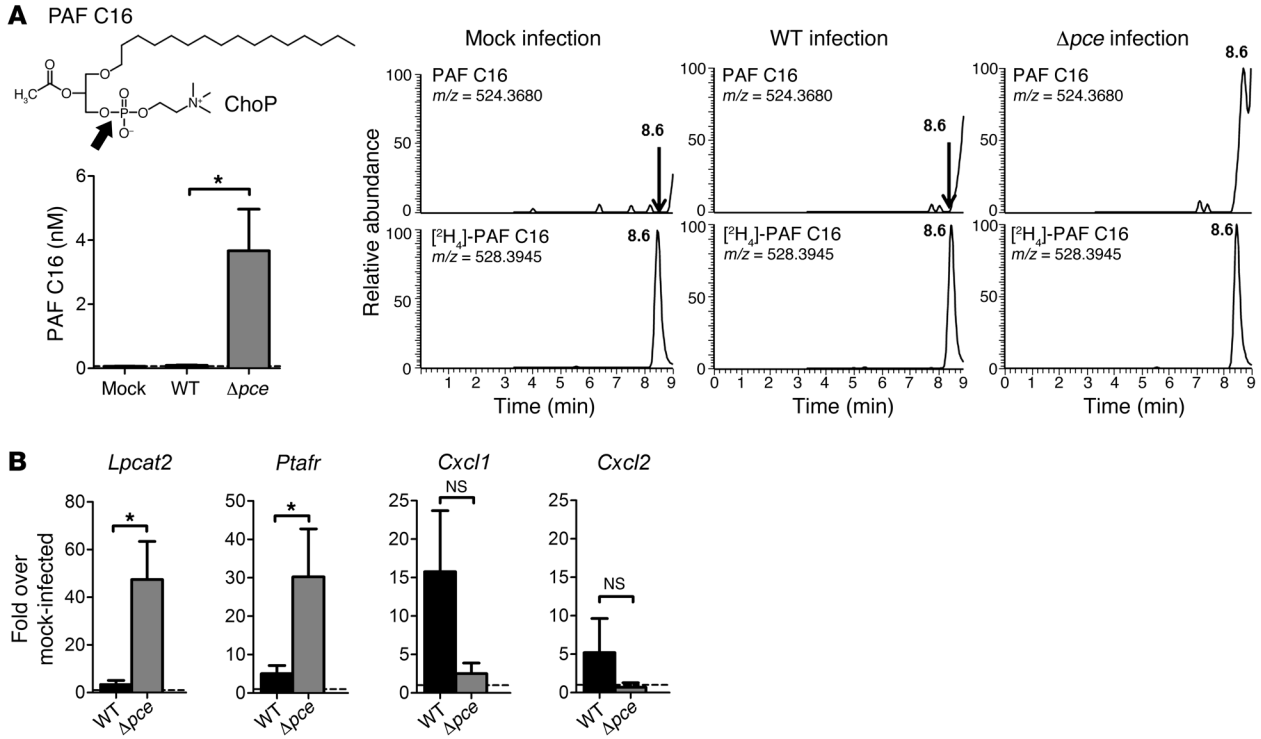

Figure 3. Pce prevents accumulation of PAF in the lumen of the upper respiratory tract, and the absence of Pce stimulates transcription of genes important for PAF signaling. (**A**) Diagram of PAF with the ChoP moiety labeled (and site of Pce-mediated hydrolysis marked with a black arrow). Detection of PAF levels in the upper airway lumen by LC-ESI/MS (limit of quantification = 0.066 nM, dashed line), quantified from pooled nasal lavages obtained from 5 mice at 3 days p.i. with PBS (Mock, white), WT (black), or Δ*pce* (gray) P1121 pneumococci. Averages reflect 3 independent biological replicates of 5 pooled mice each. Statistical significance was assessed by 1-way ANOVA with Newman-Keuls post test. For representative LC traces from lavage fluid of mock-, WT-, and Δ*pce*-infected mice, the top row displays PAF detected at 8.6 minutes' retention; the bottom row displays $^2H_4$-PAF C16–spiked control samples. (**B**) qRT-PCR measurements of relative gene expression of the PAF synthetic enzyme *Lpcat2*, PAFR (*Ptafr*), and chemokines *Cxcl1* and *Cxcl2* from nasal lavages obtained 3 days p.i. from mice colonized with PBS, WT, or Δ*pce* P1121 pneumococci (n = 6–10 mice per condition). All transcripts were normalized to GAPDH controls and are displayed relative to mice mock-infected with PBS (dotted lines). *$P < 0.05$ by Student's t test.

WT or Δ*pce* pneumococci generated from a mouse-invasive strain (serotype 6A) and tracked survival over 9 days (Figure 2A). While approximately 60% of mice infected with WT bacteria were moribund within 5 days from pneumococcal sepsis, mice inoculated with the mutant were significantly protected, suffering less than 10% lethality over the course of the experiment. This difference in survival corresponded with substantial attenuation in bacterial invasion of the bloodstream among Δ*pce* pneumococci (Figure 2B).

Δ*pce* pneumococci were similarly impaired in an infant mouse model of pneumococcal transmission (5, 48). Within litters of mice, we inoculated 1–2 "index" pups with either WT or Δ*pce* bacteria and quantified the acquisition and load of pneumococci among previously uninfected "contact" pups. In line with previous findings (48), litters exposed to WT pneumococci exhibited 64% transmission; however, only 6% of contact mice from litters exposed to Δ*pce* pneumococci acquired bacteria (Figure 2C). This corresponded with greater than 300-fold lower bacterial loads among index mice infected with the mutant. Taken together, these data provide evidence that the poor survival of Δ*pce* pneumococci in the upper airway crosses a key threshold under which disease and transmission are nearly abrogated.

Pce prevents accumulation of PAF in the upper airway lumen. Next, we analyzed the mechanism by which Pce esterase impairs neutrophil function in the upper airway. Studies using purified, recombinant enzyme have shown that Pce is capable of hydrolyzing a wide range of molecules bearing ChoP in vitro, including PAF (ref. 49 and Figure 3A, diagram). To directly quantify the impact of Pce on airway luminal PAF levels, we inoculated mice with PBS (mock) or WT or Δ*pce* pneumococci and pooled lavages from 5 mice per group on day 3 p.i. After lipid extraction and liquid chromatography (LC) to purify PAF, we subjected samples from each condition to high-resolution electrospray ionization/mass spectrometry (ESI/MS). Lavage fluid from mice inoculated with Δ*pce* bacteria harbored PAF at a concentration of approximately 3 nM, while mock- and WT-infected mice secreted no PAF detectable by LC-ESI/MS (Figure 3A), demonstrating that Pce prohibits the accumulation of PAF in the upper airway lumen during pneumococcal infection.

We also examined the expression of genes essential for PAF signaling in the airway epithelium, as PAF is known to stimulate the transcription of its own synthetic enzymes and receptor via a positive feedback loop (50, 51). At 3 days p.i. with WT or Δ*pce* bacteria, we obtained lavages with tissue lysis buffer and quantified mucosal transcripts by quantitative RT-PCR (qRT-PCR) in each condition relative to mock infection. Transcript levels of the PAF synthetic enzyme lyso-PAF acetyltransferase (*Lpcat2*) and the PAF receptor (*Ptafr*) were markedly elevated among mice infected with Δ*pce* pneumococci (Figure 3B). In contrast, transcription of neutrophil chemokines *Cxcl1* and *Cxcl2* trended lower in mice

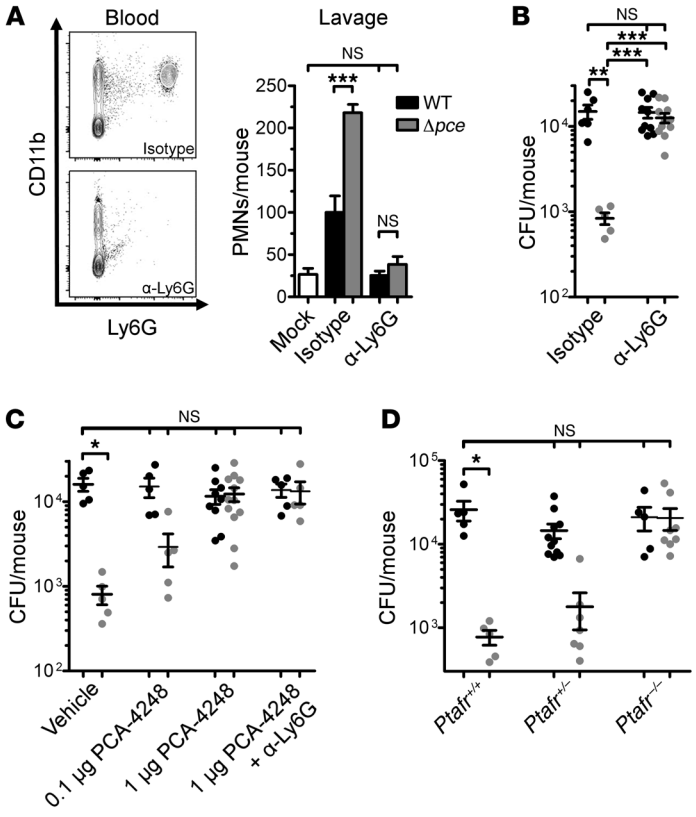

Figure 4. Pce is dispensable for pneumococcal persistence in the absence of infiltrating neutrophils or intact PAF signaling in the upper airway. (**A**) Confirmation of neutrophil depletion. Mice were treated with neutrophil-depleting antibody (α-Ly6G, clone 1A8) or IgG2a isotype control (250 μg, i.p.) on days –1, +1, and +4 p.i. with PBS (white), WT (black), or Δ*pce* (gray) P1121 pneumococci (n = 3–4 mice per condition). On day 7 p.i., depletion was confirmed by flow cytometric analysis of whole blood and nasal lavage. (**B**) Enumeration of WT (black) or Δ*pce* (gray) pneumococcal CFU obtained from nasal lavages on day 7 p.i. and after treatment of mice (n = 5–11 mice per group) with neutrophil-depleting α-Ly6G or IgG2a isotype control antibodies. (**C**) Enumeration of bacterial CFU on day 7 p.i. and after daily i.n. treatment with 0.1 or 1 μg PAFR antagonist PCA-4248 (or 1% DMSO vehicle), from days +1 to +6 p.i. (n = 5–12). The experiment was repeated with neutrophil depletion as described in **A**. (**D**) WT and Δ*pce* bacterial loads were enumerated in lavages obtained from *Ptafr*$^{-/-}$ mice and their littermate controls on day 7 p.i. (n = 5–11). *P < 0.05, **P < 0.01, and ***P < 0.001 by 1-way ANOVA with Newman-Keuls post test.

inoculated with the mutant, which is likely a consequence of lower Δ*pce* bacterial density compared with that of WT bacteria. Thus, elevation of PAF-related transcripts was not simply reflective of broad upregulation of inflammatory mediators, and Pce-mediated hydrolysis of PAF was sufficient to suppress the inflammatory feedback loop driven by PAF signaling.

Neutrophil depletion or inhibition of PAF signaling renders Pce dispensable for S. pneumoniae persistence. Our data show that *S. pneumoniae* lacking Pce esterase exhibit a survival defect during acute infection of the airway, which corresponds with elevated levels of PAF and enhanced activation of luminal neutrophils. We next asked whether neutrophils and PAF signaling play a causal role in driving the mutant's rapid clearance. To determine whether the poor survival of Δ*pce* bacteria could be rescued in the absence of infiltrating neutrophils, mice were treated with neutrophil-depleting anti-Ly6G or IgG2a isotype control antibodies on days –1, +1, and +4 after inoculation with WT or Δ*pce* pneumococci. Effective neutrophil depletion was verified in blood and nasal lavage fluid by flow cytometry (Figure 4A), and bacterial CFU from neutropenic and control mice were enumerated from nasal lavages on day 7 p.i. While the Δ*pce* mutant retained an approximately 20-fold survival defect in isotype control–treated animals, its survival was restored to WT levels in neutrophil-depleted mice (Figure 4B). This confirmed that neutrophils were required for the enhanced clearance of the mutant and that Pce esterase functions to impair neutrophil-mediated bactericidal function.

To assess whether local PAF signaling contributed to Pce-mediated neutrophil evasion, we performed the same 7-day infection with daily i.n. administration of PCA-4248, a selective antagonist of PAF receptor (PAFR) (52–54). Similar to our findings upon depletion of neutrophils, local PAFR antagonism restored survival of Δ*pce* pneumococci to levels comparable to those of WT pneumococci (Figure 4C). PCA-4248 had no direct effect on pneumococcal survival or growth in vitro (Supplemental Figure 2B). Importantly, no additional increase in the density of Δ*pce* bacteria was seen upon PCA-4248 treatment of neutrophil-depleted mice, underscoring that the predominant impact of elevated airway PAF in the absence of Pce is stimulation of neutrophil function. Last, we found that bacterial loads on day 7 p.i. were equivalent among WT and Δ*pce* pneumococci in *Ptafr*$^{-/-}$ mice (Figure 4D), providing independent evidence that augmented PAF signaling underlies the enhanced clearance of Pce-deficient bacteria. In summary, these results show that Pce esterase governs pneumococcal persistence by eliminating PAF from the airway lumen and preventing the PAF-mediated activation of neutrophils necessary for efficient pathogen clearance.

Pce esterase hydrolyzes ChoP and abrogates PAF-mediated stimulation of neutrophil function in vitro. To further clarify the mechanism by which Pce inhibits PAF-mediated neutrophil stimulation, we turned to in vitro studies using mature neutrophils isolated from murine bone marrow (BM) or human peripheral blood. We began by using bacterial-killing assays (55) to determine whether Δ*pce* pneumococci were more sensitive to neutrophils in the absence of PAF stimulation. After preincubation with complement, WT and Δ*pce* bacteria were incubated with increasing concentrations of murine or human neutrophils, and we measured bacterial survival relative to that of no-neutrophil controls. At all neutrophil concentrations tested, WT and mutant bacterial survival was equivalent (Figure 5, A and B), providing evidence that the survival defects seen in vivo were not the result of nonspecific sensitivity to neutrophil uptake. Similarly, WT and Δ*pce* pneumococci were not

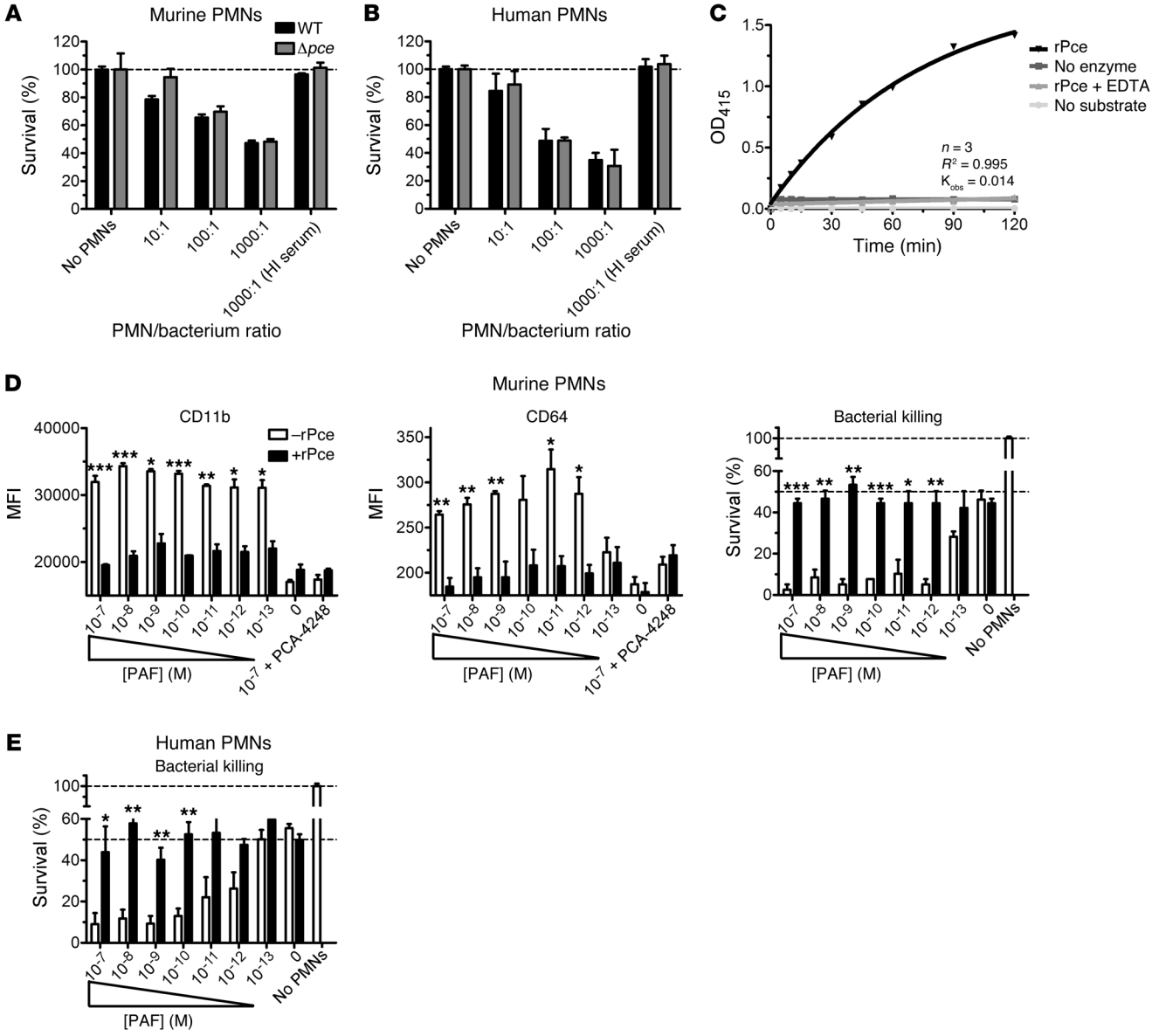

Figure 5. Pce esterase hydrolyzes ChoP from conjugated substrates and directly inhibits PAF-mediated stimulation of neutrophil activation and function in vitro. Killing of WT (black) or Δ*pce* (gray) P1121 pneumococci in vitro by murine (**A**) or human (**B**) neutrophils at the indicated neutrophil/bacterium ratios, after preopsonization with BRS. Bacterial survival was measured relative to control assays in the absence of neutrophils (dotted line). HI, heat inactivated. (**C**) Kinetic time course of *p*-nitrophenol liberation (absorbance at 415 nm) after incubation of pNPPC with recombinant Pce enzyme (rPce, black line). Assays were repeated in the absence of Pce enzyme or pNPPC substrate or in the presence of 250 mM EDTA. K_{obs}, observed kinetic rate constant. (**D**) MFI quantification of bacterial uptake receptors CD11b and CD64 on murine neutrophils treated with PAF that was preincubated with rPce (black) or PBS (white). PAF stimulation assays were repeated with 10^{-5} M of the PAFR antagonist PCA-4248 as a specificity control. Killing assays using WT pneumococci (PMN/bacterium ratio, 1,000:1) were performed after PAF-mediated murine (**D**) or human (**E**) neutrophil stimulation in the presence (black) or absence (white) of rPce. Top dotted line denotes 100% bacterial survival; bottom dotted line denotes average survival in the absence of PAF. For all panels, data averages reflect at least 3 independent experiments (3–4 independent biological replicates for cellular assays). *$P < 0.05$, **$P < 0.01$, and ***$P < 0.001$ by Student's *t* test for all pairwise comparisons.

significantly different in terms of growth characteristics in vitro (Supplemental Figure 2A), sensitivity to complement deposition (Supplemental Figure 3A), capsule expression levels (Supplemental Figure 3B), or cell surface ChoP accessibility (Supplemental Figure 3C) as assessed by bacterial flow cytometry.

Using recombinant Pce esterase (rPce), we next confirmed that the enzyme bears efficient ChoP hydrolysis activity upon incubation with chromogenic substrate *p*-nitrophenylphosphorylcholine (pNPPC), which yields *p*-nitrophenol upon removal of its ChoP moiety (Figure 5C) (56). To assess whether rPce directly inhibits PAF-mediated stimulation of neutrophils, we pretreated PAF at a range of physiologic concentrations centered around 3 nM (the concentration detected by ESI/MS) with rPce enzyme or PBS control. We applied the conditioned PAF media to the phagocytes and quantified upregulation of CD11b and CD64 receptor expression on murine neutrophils by flow cytometry (Figure 5D).

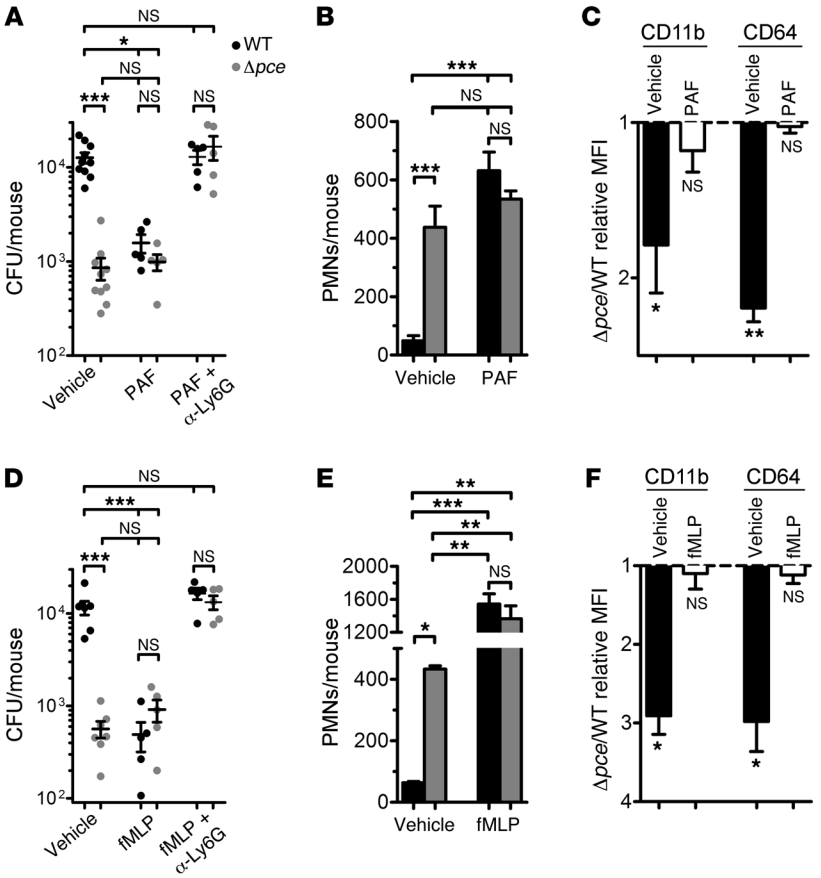

Figure 6. Exogenous stimulation of neutrophils in situ overwhelms Pce-mediated immune evasion. (**A**) Enumeration of WT (black) or Δ*pce* (gray) pneumococcal CFU obtained on day 7 p.i. and after daily (+1 to +6) i.n. treatments with 1 μg PAF or vehicle control (1% DMSO in PBS). The experiment was repeated after treatment with neutrophil-depleting α-Ly6G or IgG2a isotype control antibody (see Figure 4B) (n = 5–10 mice per condition). (**B**) Quantification of neutrophils elicited by WT (black) or Δ*pce* (gray) P1121 pneumococci in nasal lavages of vehicle- or PAF-treated mice on day 7 p.i. (n = 5 per group). (**C**) Relative MFI of uptake receptor expression on luminal neutrophils elicited by WT or Δ*pce* pneumococci (Δ*pce*/WT) after daily treatment with vehicle (black) or 1 μg PAF (white), as described in **A** (n = 5). (**D**) Enumeration of bacterial CFU as in **A**, with and without daily i.n. treatment with 1 μg fMLP or vehicle (n = 5–7). (**E**) Quantification of elicited neutrophils as in **B**, with or without treatment with fMLP (n = 5). (**F**) Relative MFI of uptake receptor expression on neutrophils elicited by WT or Δ*pce* pneumococci (Δ*pce*/WT) after daily treatment with vehicle (black) or 1 μg fMLP (white), as in **C** (n = 5). Statistical significance was assessed by 1-way ANOVA with Newman-Keuls post test, except for **C** and **F**, wherein significance was assessed by 1-sample Student's t test relative to a value of 1. $^*P < 0.05$, $^{**}P < 0.01$, $^{***}P < 0.001$.

While increasing PAF concentrations correlated with upregulation of both receptors under the PBS control condition, no such correlation was seen if PAF was preincubated with rPce. Similarly, pretreatment of PAF with rPce abrogated the increased killing capacity conferred when PAF was applied to murine or human neutrophils (Figure 5, D and E). Collectively, these findings reveal that Pce functions to hydrolyze ChoP from conjugated substrates, and its processing of PAF directly inhibits neutrophil activation and phagocyte function.

Exogenous stimulation of neutrophils in situ overwhelms Pce-mediated immune evasion. Having established that Pce inhibits acute clearance of *S. pneumoniae* in vivo by depriving neutrophils of an essential stimulatory ligand, we posited that this immune evasion mechanism could be overcome if luminal neutrophils were sufficiently activated. We tested this by performing 7-day WT and Δ*pce* pneumococcal infection experiments with daily i.n. treatment with an excess of either PAF or *N*-formyl-Met-Leu-Phe (fMLP), a bacterial peptide that stimulates neutrophil chemotaxis and activation through pathways distinct from those of PAF (39, 57). At day 7 p.i., mice inoculated with WT pneumococci and treated with PAF (Figure 6A) or fMLP (Figure 6D) exhibited significantly enhanced clearance, such that WT bacterial loads resembled that of Δ*pce*, while the mutant's survival was not substantially affected upon stimulant treatment. PAF and fMLP exerted no detectable effect on pneumococcal growth or viability in vitro (Supplemental Figure 2, C and D).

Critically, repeating these treatments after systemic neutrophil depletion restored survival of both pneumococcal strains to levels seen for WT bacteria in mice treated with vehicle controls (Figure 6, A and D), reinforcing that neutrophils were responsible for the observed increase in clearance. Enhancement of WT pneumococcal clearance upon PAF treatment corresponded with an increase in the number of neutrophils in the airway lumen to levels similar to those seen during Δ*pce* infection. In contrast, neutrophil numbers elicited by Δ*pce* pneumococci were unaffected by PAF administration (Figure 6B). These results suggested that introduction of excess PAF ligand overwhelmed the capability of Pce esterase to mediate immune evasion for WT bacteria, yielding neutrophil phenotypes and bacterial survival that mimicked infection in the absence of Pce. Consistent with its known role as a strong chemoattractant (58), fMLP treatment stimulated a substantial elevation in airway neutrophil recruitment, but neutrophil numbers were again equalized among WT- and Δ*pce*-infected mice (Figure 6E). Last, flow cytometric analysis of luminal neutrophils revealed that treatment with PAF or fMLP enhanced the relative expression of CD11b and CD64 on cells elicited by WT pneumococci to levels seen in those recruited by Δ*pce*, abrogating the relative difference in activation observed in the absence of stimulation in situ (Figure 6, C and F). Taken together, these results serve to reinforce that Pce promotes pneumococcal persistence through fine regulation of neutrophil activation and that clearance of WT bacteria can be substantially accelerated by stimulating neutrophil function.

Subversion of PAF signaling is conserved in Haemophilus influenzae, another ChoP-expressing pathogen of the airway. We sought to determine whether exploitation of ChoP mimicry to suppress PAF represents a conserved mechanism among other ChoP-expressing bacterial pathogens. We focused on *Haemophilus influenzae*,

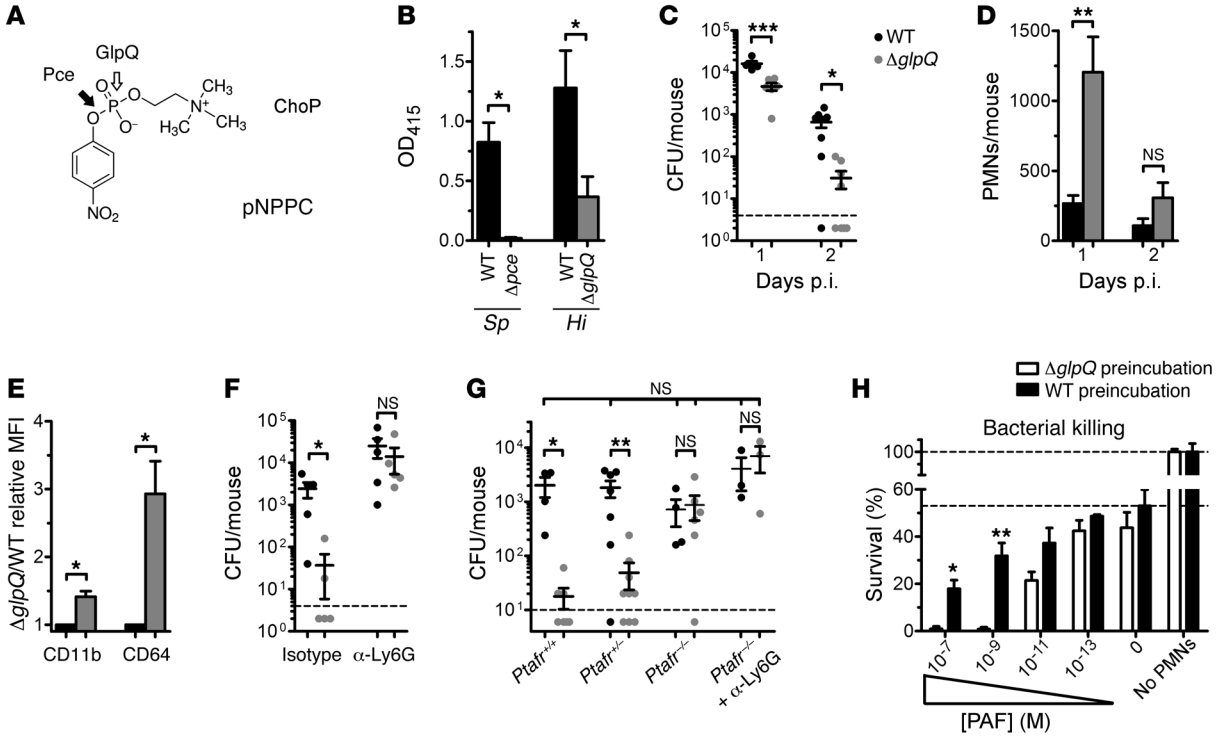

Figure 7. *H. influenzae* GlpQ hydrolyzes ChoP and contributes to evasion of PAF-mediated neutrophil defense of the airway. (**A**) Diagram of pNPPC. Black arrow denotes the site of hydrolysis by *S. pneumoniae* Pce; white arrow indicates hydrolysis by *H. influenzae* GlpQ. (**B**) *p*-nitrophenol liberation after incubating pNPPC with WT (black) or mutant (gray) *S. pneumoniae* (*Sp*) or *H. influenzae* (*Hi*) ($n = 5$). (**C**) Survival of WT (black) or Δ*glpQ* (gray) *H. influenzae* during infection of the murine upper airway ($n = 5$–8 mice per group, LOD = 4). (**D**) Quantification of neutrophils obtained from mice inoculated with WT or Δ*glpQ* bacteria ($n = 4$). (**E**) CD11b and CD64 relative MFI on neutrophils elicited by WT or Δ*glpQ* bacteria, day 2 p.i. ($n = 4$). (**F**) Enumeration of day-2 WT or Δ*glpQ H. influenzae* CFU after treatment with α-Ly6G antibody or IgG2a isotype control ($n = 5$, LOD = 4). (**G**) WT and Δ*glpQ* bacterial loads from *Ptafr*$^{-/-}$ mice, littermate controls, or neutropenic *Ptafr*$^{-/-}$ mice on day 2 p.i. ($n = 3$–9, LOD = 10). (**H**) Bacterial killing assay of WT *H. influenzae* by 1,000:1 murine neutrophils pretreated with increasing concentrations of conditioned PAF media; PAF was preincubated with heat-killed WT (black) or Δ*glpQ* (white) bacteria before mixing with neutrophils for killing assays. Average values represent 3 biological replicates. Top dotted line: 100% bacterial survival; bottom dotted line: average survival in the absence of PAF. Statistical significance was assessed by Student's *t* test for pairwise comparisons (**B** and **H**); 1-way ANOVA with Newman-Keuls post test for multigroup comparisons (**C**, **D**, **F**, and **G**); and 1-sample Student's *t* test relative to null = 1 for relative MFI measurements (**E**). $^*P < 0.05$, $^{**}P < 0.01$, $^{***}P < 0.001$.

as it displays ChoP on surface-exposed lipooligosaccharide chains (28), remains an important cause of respiratory disease worldwide (59, 60), and could be investigated using a murine model of upper respiratory tract infection (61). No direct homologs for pneumococcal Pce were apparent in *H. influenzae* by sequence analysis. However, previous work from our laboratory suggested that the highly conserved, surface-bound phosphodiesterase lipoprotein GlpQ (also known as protein D) bears the ability to efficiently hydrolyze ChoP from conjugated substrates (62). Previously ascribed a role in bacterial acquisition of choline from host cells, GlpQ has long been known to be important for virulence during mucosal infection, though the nature of its contribution has remained incompletely understood (63). We hypothesized that this ChoP-binding enzyme functioned analogously to pneumococcal Pce esterase and contributed to PAF evasion during airway infection.

To confirm previous reports that GlpQ contributes to hydrolysis of ChoP (62), we applied WT and Δ*glpQ H. influenzae* to chromogenic pNPPC assays and measured absorbance after 120 minutes compared with that generated by WT and Δ*pce* pneumococci (Figure 7, A and B). Note that GlpQ cleaves ChoP at the phosphoester bond proximal to choline and therefore requires the addition of exogenous alkaline phosphatase enzyme to reactions for chromogenic activity in this assay (Figure 7A, arrows). Similar to the results for Δ*pce* pneumococci, ChoP hydrolysis activity by *H. influenzae* was significantly impaired in the absence of GlpQ, though some residual activity remained (Figure 7B). These results confirmed that native GlpQ hydrolyzes ChoP efficiently.

We next asked whether GlpQ contributes to bacterial persistence in murine upper airway infection. Mice inoculated with WT or Δ*glpQ H. influenzae* were sacrificed on days 1 and 2 p.i. for bacterial enumeration. By day 2, Δ*glpQ* bacteria exhibited a survival defect exceeding 20-fold (Figure 7C). Flow cytometric analyses of lavage fluid suggested enhanced influx of neutrophils during acute infection with the Δ*glpQ* mutant compared with that observed for WT bacteria (Figure 7D), and neutrophils elicited by the mutant exhibited significantly elevated bacterial uptake receptor expression by day 2 p.i. (Figure 7E). To establish whether neutrophils drive Δ*glpQ* persistence defects, we repeated 2-day infections after anti-Ly6G or IgG2a isotype antibody treatments on days –1 and +1 after inoculation. Akin to results observed with Δ*pce* pneumococci, neutropenia rescued Δ*glpQ* survival such that it resembled that of WT *H. influenzae* (Figure 7F). Δ*glpQ* survival was also rescued

in *Ptafr*$^{-/-}$ mice, while littermate control mice recapitulated the mutant defect seen previously, indicating that intact PAF signaling is essential for enhanced bacterial clearance in the absence of GlpQ (Figure 7G). Importantly, neutropenia did not lead to significantly enhanced bacterial survival in *Ptafr*$^{-/-}$ mice, suggesting that PAF stimulation plays an important role in regulating neutrophil function during *H. influenzae* infection of the airway. Collectively, these findings reveal that GlpQ is critical for limiting neutrophil responses in vivo through inhibition of PAF signaling.

Last, we performed neutrophil bactericidal assays in vitro to assess whether preincubation of PAF with *H. influenzae* bearing GlpQ hindered its ability to stimulate neutrophil-mediated phagocytic function when compared with preincubation with Δ*glpQ* bacteria. We mixed neutrophils pretreated with each enzyme-conditioned PAF solution with preopsonized WT *H. influenzae* and quantified bacterial survival over a range of PAF concentrations compared with no-PAF and no-neutrophil controls (Figure 7H). While evidence of PAF-mediated stimulation of phagocytosis remained evident after pretreatment in either condition, this enhancement of killing was impaired significantly when neutrophils were prestimulated with WT bacteria (black bars) compared with Δ*glpQ* mutant (white bars). These results reinforce that GlpQ directly inhibits the effects of PAF on neutrophil activity.

Discussion

Evasion of neutrophil-mediated phagocytosis is essential for the mucosal persistence of extracellular bacterial pathogens, and mounting evidence suggests that direct suppression of neutrophil activation plays an important role in mediating microbial escape from acute inflammatory responses. Here, we showed that enzymatic degradation of PAF, driven by ChoP mimicry, underlies neutrophil subversion by *S. pneumoniae* and *H. influenzae* in the upper airway. As stable infection of the upper airway is a prerequisite for the development of pneumonia and sepsis for many respiratory pathogens, a mechanistic understanding of immune evasion in this niche is particularly important for developing interventions designed to prevent the transition from asymptomatic carriage to invasive disease (64).

We found that the surface-bound ChoP esterase Pce governed the exploitation of ChoP mimicry essential for pneumococcal persistence. The near-universal conservation of Pce among pneumococcal clinical isolates (65) and results from early animal studies (66) support the idea that the enzyme contributes to bacterial fitness during airway infection, but the nature of its function in vivo has been less clear. Most studies characterizing Pce activity have focused on its ability to remodel the pneumococcal cell wall by hydrolyzing ChoP residues from teichoic acid chains, a function associated with enhanced adhesion to epithelial surfaces (49, 56). However, Pce-deficient pneumococci exhibit essentially unaltered epithelial adherence properties, and the enzyme is unable to hydrolyze more than 30% of ChoP residues from these substrates, even in saturating conditions (66, 67). Our findings reveal that exploitation of shared ChoP moieties allows degradation of host-derived PAF, rather than modifications to the cell wall, to be the major contribution of Pce to immune evasion during respiratory infection.

Using direct measurement of PAF by high-resolution LC-ESI/MS, we tested the hypothesis that Pce restricts PAF accumulation during infection. In upper airway lavage fluid, PAF was detectable only from mice infected with Pce-deficient bacteria, at a concentration of approximately 3 nM. Even if the dilution inherent to lavage is discounted, this concentration exceeded the dissociation constant of PAFR on leukocytes (37, 68) and mimicked the PAF levels observed in the inflamed human airway (69). Together, this reinforced that PAF accumulated to a level that was sufficient to effectively stimulate neutrophils in the airway. The product of PAF hydrolysis by Pce, 1-*O*-hexadecyl-2-*O*-acetyl-sn-glycerol, was not detectable in any condition tested, possibly reflecting rapid degradation in vivo. Additionally, we showed that Pce directly suppressed PAF-mediated stimulation of human and murine neutrophil bactericidal function upon ex vivo treatment with physiologically relevant concentrations of PAF, further supporting that Pce limits PAF levels through enzymatic degradation.

We focused our investigations entirely on PAF C16 (1-*O*-hexadecyl-2-*O*-acetyl-*sn*-glyceryl-3-phosphorylcholine), the most abundant and well-characterized member of a diverse set of PAF-like lipids secreted during inflammation. While some PAF-like lipids can stimulate neutrophil bactericidal capacity, nearly all bind most avidly to receptors other than PAFR (70). A number of studies have shown that even small modifications to the molecular structure of PAF significantly disrupt its binding and signaling potency through its cognate receptor (71). Since we found that the enhanced neutrophil activation observed during infection with *Δpce* pneumococci was abrogated entirely upon PAFR blockade in vivo or when using PAFR-deficient mice, we concentrated our analyses on PAF. Whether other PAF-like lipids are regulated similarly by Pce during pneumococcal infection remains a subject of ongoing investigation.

Our work demonstrated that Pce-mediated PAF degradation results in functional impairment of neutrophils responding to pneumococcal infection, rendering them unable to mediate efficient phagocytosis. Recent studies have suggested that, in addition to suppressing clearance, recruiting an ineffective acute inflammatory response can be directly beneficial for bacterial fitness. Increased mucus production can provide nutrients to stimulate bacterial growth at mucosal surfaces (72), inflammatory influxes can enhance bacterial shedding from the nasopharynx to promote transmission between hosts (48), and the recruitment of neutrophils can provide an inflammatory milieu that may neutralize bacterial competitors among the flora (9). These advantages rely on phagocytes that alter the mucosal environment without presenting significant bactericidal pressure. For the pneumococcus, Pce-mediated neutrophil suppression may constitute a central mechanism through which inflammation can be utilized to the advantage of the microbe.

A wide range of extracellular bacteria display ChoP on their surfaces and express enzymes that govern ChoP hydrolysis and turnover, suggesting that other pathogens may harbor unappreciated strategies for evading clearance through mimicry-driven degradation of PAF (28). Along with the pneumococcus, *H. influenzae*, *Neisseria meningitidis*, and *Neisseria gonorrheae* carry ChoP as surface modifications, and most of these pathogens use ChoP to bind PAFR directly, reflecting a common strategy of passive, structural mimicry of PAF (73–75). Our work implies that active, enzymatic mechanisms exploiting ChoP mimicry may underlie the well-described resistance of these organisms to neutrophils and may expose a broadly applicable target for therapeutic intervention. To

this end, we investigated neutrophil evasion by *H. influenzae* in the upper airway. Despite bearing no apparent homologs for Pce, we found that *H. influenzae* harbors an analogous mechanism for mimicry-driven, enzymatic subversion of PAF through ChoP hydrolysis by the surface-bound phosphodiesterase GlpQ. The functional similarity of these structurally unrelated esterases, used by disparate pathogens occupying the same upper airway niche, suggests that PAF-mediated inflammation may have necessitated convergent evolution (27) aimed at manipulating and neutralizing PAF activity to achieve fitness in the airway environment. Our findings also suggest that GlpQ does not govern the entirety of ChoP hydrolytic activity mediated by *H. influenzae*, as some residual enzymatic activity persists among Δ*glpQ* mutants. The identity and functions of these other contributors remain under investigation.

The central importance of regulating PAF-mediated inflammation is further exemplified by microbes that do not express ChoP but disrupt PAF signaling by means other than molecular mimicry. *Staphylococcus aureus* has been shown to bind leukocytes and platelets and directly modulate PAFR signaling (76, 77). *Streptococcus pyogenes* uses a secreted enzyme to cleave acetyl groups from PAF ligand and inhibit neutrophil chemotaxis during invasive skin infection (78). It remains conceivable that additional mechanisms for PAF disruption by *S. pneumoniae* and *H. influenzae* exist independently of ChoP hydrolysis activity. Together, this emphasizes that microbial manipulation of PAF signaling may be critical for successful immune evasion and that targeting convergent bacterial strategies to this end may be a promising avenue for antimicrobial interventions.

The tight regulation of PAF signaling mediated by the pneumococcus and other extracellular bacteria suggests that these neutrophil evasion mechanisms could be overcome if PAF levels are elevated sufficiently at the site of infection. Accordingly, we found that stimulating neutrophils in situ during pneumococcal infection with excess PAF restored their activation state and phagocytic capacity, resulting in enhanced bacterial clearance. This implies that a threshold concentration of PAF may define the balance between effective bacterial evasion and neutrophil-mediated clearance. While delivering PAF itself is unlikely to be a clinically tractable method to overcome such a threshold, targeting host-encoded negative feedback mechanisms that regulate PAF levels may be more promising. Lipoprotein-associated phospholipase A_2, also known as PAF acetylhydrolase, is secreted by the host, has been shown to mediate PAF hydrolysis, and can dampen PAF-mediated inflammation in vivo (79). It is released into the upper airway lumen during respiratory inflammation and has been shown to be upregulated during pneumococcal infection, and clinical trials have demonstrated that an antagonist, darapladib, is safe in humans (80–82). While studies aimed to assess the effectiveness of targeting PAF acetylhydrolase in combating pneumococcal and other bacterial infections are ongoing, this may serve as an important example of how mechanistic investigations of bacterial immune evasion may reveal rational targets for host-directed antimicrobial therapies.

Methods

Bacterial strains. *S. pneumoniae* strains P1121 (type 23F clinical isolate), TIGR4 (type 4 isolate), and P1547 (a mouse-virulent type 6A isolate) were grown in tryptic soy (TS) broth at 37°C to mid-log phase, as described previously (19, 83, 84). Mutants lacking ChoP esterase (*Δpce*) were derived for each strain from an insertion-duplication mutant (56) and used for all experiments except where specified. Independently, we created an in-frame, unmarked *Δpce*-deletion mutant and a genetically corrected revertant (*Δpce::pce*) by previously described methods (41). Refer to the Supplemental Methods for details and to Supplemental Table 1 for primers used in mutagenesis. Spontaneously streptomycin-resistant isolates of *H. influenzae* Eagan (a type b encapsulated strain) and an isogenic mutant lacking the surface phosphodiesterase GlpQ (*ΔglpQ*) were used as described previously (62). *H. influenzae* was grown to mid-log phase shaking at 37°C in brain-heart infusion (BHI) broth supplemented with 2% Fildes Enrichment (Thermo Scientific) and 2 μg/ml β-NAD (Sigma-Aldrich) (sBHI).

Murine model of upper airway infection. Six- to eight-week-old C57BL/6 mice were obtained from The Jackson Laboratory. PAFR-deficient (*Ptafr*$^{-/-}$) mice on a C57BL/6 background (*Ptafr*^{tm1Eit}) were a gift of Elaine Tuomanen (St. Jude Children's Research Hospital, Memphis, Tennessee, USA) (85, 86). All KO mice were bred from heterozygotes and compared with littermate controls. For upper airway infection with *S. pneumoniae* or *H. influenzae*, mice were inoculated i.n. with 10^7 CFU of mid-log phase bacteria suspended in 10 μl sterile PBS. To prevent aspiration of the inoculum from the upper airway into the lungs, mice were not anesthetized during inoculation. We obtained upper airway lavages upon sacrifice through tracheal cannulation and expression of 200 μl sterile PBS through the nares. Lavage samples from pneumococcal infections were plated on TS agar supplemented with 5 to 20 μg/ml neomycin and 5,000 U catalase per plate (Worthington Biochemical). To discern insertion-derived and in-frame deletion *Δpce* mutants from WT pneumococci, plates were supplemented with 1 μg/ml erythromycin or 200 μg/ml streptomycin, respectively. Lavage samples from mice infected with *H. influenzae* were plated on sBHI agar supplemented with 100 μg/ml streptomycin. *ΔglpQ* mutants were discerned from WT *H. influenzae* by supplementation with 20 μg/ml kanamycin. CFU counts were enumerated by quantitative culture after overnight incubation at 37°C in 5% CO_2 (72).

Flow cytometry. Nasal lavages were pelleted at 1,200 *g* for 5 minutes and resuspended in PBS containing 1% BSA. FcR blocking was achieved with 1:100 dilution of anti-CD16/32 (clone 2.4G2; BD Biosciences), and cell viability was assessed by staining with Fixable Viability Dye eFluor 780 (eBioscience) according to the manufacturer's instructions. Neutrophils were immunophenotyped by staining with fluorophore-conjugated antibodies (diluted 1:150) against the following surface markers: CD45 (clone 30-F11; eBioscience); Ly6G (clone 1A8; BioLegend); CD11b (clone M1/70; BioLegend); CD64 (clone X54-5/7.1; BioLegend); and CD62L (clone MEL-14; BioLegend). Neutrophil ROS were quantified after incubation with 10 μM CM-H_2DCFDA (Life Technologies) according to the manufacturer's instructions (87, 88). All cytometry was performed using a BD LSR II flow cytometer and analyzed with FlowJo software.

Bacterial transmission model. Infant mouse pneumococcal transmission experiments were performed as described previously (5, 48). On day 4 of life, we inoculated 1–2 index pups per litter (approximately 1 in 4) with 2,000 CFU of *S. pneumoniae* strain P1121 in 3 μl PBS. On day 8 of life, all pups were infected i.n. with 2×10^4 $TCID_{50}$ influenza A strain HKx31, as influenza coinfection is required for pneumococcal

transmission between mice (89). On day 14, all pups were sacrificed, and upper airway bacterial loads were quantified among index and previously uninfected contact mice.

LC-ESI/MS quantification of PAF from the murine upper airway lumen. PAF-C16 was extracted and quantified from murine upper airway lavage fluid pooled from 5 mice per condition on day 3 of infection (performed in triplicate). Briefly, 0.5 ml lavage fluid was spiked with 2 ng deuterated PAF-C16-d4 (Cayman Chemical) as a quantification standard, extracted in methanol with shaking, and resuspended in isopropanol/acetonitrile/water (3:5:2; v/v/v). Reverse-phase separations of 3-μl injections were conducted using a nano-ACQUITY UPLC system and XBridge BEH130 C18 column (Waters Corp.) at 1.5 μl/minute. High-resolution LC-ESI/MS quantification was performed using a recently calibrated LTQ XL-Orbitrap hybrid mass spectrometer (Thermo Scientific) in positive ion mode and with a Michrom captive spray ESI source. Data analysis was performed using Xcalibur software (Thermo Scientific) from raw mass spectral data.

qRT-PCR. RNA was extracted from the upper airway mucosa through lavage with 500 μl RLT lysis buffer (QIAGEN) (90). After isolation of total RNA (RNeasy Kit; QIAGEN), cDNA was generated using the High-Capacity cDNA Reverse Transcription Kit (Applied Biosystems), and qRT-PCR was performed using 10 ng cDNA, 0.5 μM primers, and SYBR Green Master Mix (Life Technologies). Differential RNA expression was quantified using the ΔΔCt method relative to *Gapdh* transcript levels. qRT-PCR primer sequences are listed in Supplemental Table 1.

Neutrophil depletion and i.n. drug treatments. Systemic depletion of murine neutrophils was achieved by i.p. injection of 250 μg anti-Ly6G antibody (clone 1A8; Bio X Cell) or IgG2a isotype control antibody (clone 2A3; Bio X Cell) at the indicated time points (Results and Figures 4 and 6). Neutropenia was confirmed by flow cytometry and microscopic inspection using Shandon Kwik-Diff stains (Thermo Scientific). For i.n. drug treatments, 0.1 or 1 μg PAF (Cayman Chemical), PAF receptor antagonist PCA-4248 (Tocris), or fMLP (Sigma-Aldrich) was instilled daily (days 1–6), suspended in 10 μl sterile PBS. Vehicle control experiments used dilutions of drug solvent (DMSO) in PBS identical to those for drug dilutions.

Generation of rPce. rPce protein was produced as described previously (56), with modifications. *pce* was cloned from the P1121 *S. pneumoniae* genome with primers that introduced flanking restriction sites for *BamHI* and *SacI* (New England BioLabs Inc.) (see Supplemental Table 1). After restriction digestion and gel purification, the *pce* fragment was cloned into pET28a (Novagen) using T4 DNA ligase (New England BioLabs Inc.) to generate a construct in which *pce* was flanked with N- and C-terminal hexa-histidine tags. Ligated product was transformed into XL-1 Blue competent *E. coli* (Agilent), amplified, and purified by plasmid miniprep (Sigma-Aldrich). After sequence confirmation, *pce*-pET28a was transformed into BL21 (DE3)pLysS competent cells (Promega), and protein expression was induced according to the manufacturer's instructions with 1 mM isopropyl β-D-thiogalactopyranoside (IPTG). Native cell lysis was achieved by sonication on ice, and lysates were applied to a Ni-NTA purification column (GE Healthcare Life Sciences) by fast protein LC (FPLC), followed by dialysis against 20 mM HEPES with 3 μM zinc sulfate.

Chromogenic assay for ChoP hydrolysis. Pce catalytic activity was assessed by incubation of 4 μg enzyme with 21 μg of the chromogenic substrate pNPPC (Sigma-Aldrich) at 37°C in 200 μl. Absorbance at 415 nm was monitored at the indicated time points (Figure 5C and Results) to detect ChoP hydrolysis and the resultant liberation of *p*-nitrophenol (56). For chromogenic assays using whole bacteria and isogenic mutants, 50 μl OD_{620} 1.0 normalized bacteria was resuspended in potassium phosphate buffer (pH 8.0) and incubated with pNPPC, as above, for 120 minutes. For reactions testing *H. influenzae* strains, 1 U shrimp alkaline phosphatase (Affymetrix) was included in the assays to cleave terminal phosphate groups remaining after GlpQ hydrolysis.

Isolation of neutrophils from murine BM and human peripheral blood. Mature murine neutrophils were flushed from murine femora and washed with Hank's Balanced Salt Solution buffer with calcium (Mediatech) containing 0.1% gelatin before enrichment with a discontinuous gradient of Histopaque-1077 and -1119 (Sigma-Aldrich). Flow cytometry confirmed that more than 90% of the $CD45^+$ cells isolated were $Ly6G^+CD11b^+$. Human neutrophils were obtained from healthy donors and isolated by Polymorphprep (Axis Shield) gradient centrifugation as described previously (91).

Neutrophil activation and bactericidal assays. To assess the impact of Pce on PAF-stimulated neutrophil function, we performed assays using murine and human neutrophils ex vivo. Purified PAF (Cayman Chemical) was incubated in the presence or absence of 4 μg recombinant Pce in 100 μl potassium phosphate buffer (100 mM, pH 7.4) for 20 minutes at 37°C. Reaction products were applied to 10^5 murine or 10^4 human freshly isolated neutrophils at a 1:1 dilution and allowed to incubate for 30 minutes. All values listed for PAF represent final concentrations after incubation with neutrophils. Murine neutrophil activation was assessed by flow cytometric analysis of CD11b and CD64 as described above. Assays for neutrophil opsonophagocytic killing were performed as described previously (55, 84); 10^2 bacteria were preopsonized for 30 minutes with baby rabbit serum (BRS) as a complement source and applied to PAF-treated neutrophils at the indicated bacterium/phagocyte ratios (Figure 5, A, B, and D, and Figure 7H). Refer to the Supplemental Methods for details on neutrophil bactericidal assays involving *H. influenzae*.

Statistics. All data are presented as the mean ± SEM. Data were analyzed using a 2-tailed Student's *t* test for comparisons between 2 groups and ANOVA with Newman-Keuls post test for all comparisons of more than 2 groups. Relative mean fluorescence intensity (MFI) measurements were analyzed using pairwise 1-sample Student's *t* tests relative to a null ratio of 1. For all analyses, $P < 0.05$ was considered statistically significant.

Study approval. All animal experiments were approved by and performed in strict accordance with the guidelines of the IACUC of the University of Pennsylvania.

Acknowledgments

We thank Jan Erikson (Wistar Institute) for providing influenza strains, Amanda Hay and Jun Zhu for assistance with kinetic bacterial growth assays, and Young Hwang, Jay Gardner, and Michael Betts for assistance with FPLC and protein purification. This work was supported by NIH grants AI038446, AI105168, and AI060516 (to J.N. Weiser) and P30CA016520 (to I.A. Blair).

Address correspondence to: Jeffrey N. Weiser, Medical Science Building, Room 256, 550 First Avenue, New York, New York 10016, USA. Phone: 212.263.1080; E-mail: Jeffrey.Weiser@nyumc.org.

1. Kolaczkowska E, Kubes P. Neutrophil recruitment and function in health and inflammation. *Nat Rev Immunol.* 2013;13(3):159–175.
2. Amulic B, Cazalet C, Hayes GL, Metzler KD, Zychlinsky A. Neutrophil function: from mechanisms to disease. *Annu Rev Immunol.* 2011;30:459–489.
3. Segal AW. How neutrophils kill microbes. *Annu Rev Immunol.* 2004;23:197–223.
4. Mantovani A, Cassatella MA, Costantini C, Jaillon S. Neutrophils in the activation and regulation of innate and adaptive immunity. *Nat Rev Immunol.* 2011;11(8):519–531.
5. Short KR, Reading PC, Wang N, Diavatopoulos DA, Wijburg OL. Increased nasopharyngeal bacterial titers and local inflammation facilitate transmission of Streptococcus pneumoniae. *mBio*. 2011;3(5):e00255-12.
6. Urban CF, Lourido S, Zychlinsky A. How do microbes evade neutrophil killing? *Cell Microbiol.* 2006;8(11):1687–1696.
7. Sarantis H, Grinstein S. Subversion of phagocytosis for pathogen survival. *Cell Host Microbe.* 2012;12(4):419–431.
8. Sadik CD, Kim ND, Luster AD. Neutrophils cascading their way to inflammation. *Trends Immunol.* 2011;32(10):452–460.
9. Maekawa T, et al. Porphyromonas gingivalis manipulates complement and TLR signaling to uncouple bacterial clearance from inflammation and promote dysbiosis. *Cell Host Microbe.* 2014;15(6):768–778.
10. Spaan AN, Surewaard BG, Nijland R, van Strijp JA. Neutrophils versus Staphylococcus aureus: a biological tug of war. *Annu Rev Microbiol.* 2012;67: 629–650.
11. Wood WB, Smith MR, Watson B. Studies on the mechanism of recovery in pneumococcal pneumonia: IV. The mechanism of phagocytosis in the absence of antibody. *J Exp Med*. 1946;84(4):387–402.
12. Wood WB, Smith MR. Host-parasite relationships in experimental pneumonia due to pneumococcus type III. *J Exp Med*. 1950;92(1):85–100.
13. Knecht JC, Schiffman G, Austrian R. Some biological properties of Pneumococcus type 37 and the chemistry of its capsular polysaccharide. *J Exp Med*. 1970;132(3):475–487.
14. O'Brien KL, et al. Burden of disease caused by Streptococcus pneumoniae in children younger than 5 years: global estimates. *Lancet*. 2009;374(9693):893–902.
15. Griffin MR, Zhu Y, Moore MR, Whitney CG, Grijalva CG. U.S. hospitalizations for pneumonia after a decade of pneumococcal vaccination. *N Engl J Med*. 2013;369(2):155–163.
16. Simell B, et al. The fundamental link between pneumococcal carriage and disease. *Expert Rev Vaccines.* 2012;11(7):841–855.
17. Gray BM, Converse GM, Dillon HC. Epidemiologic studies of Streptococcus pneumoniae in infants: acquisition, carriage, and infection during the first 24 months of life. *J Infect Dis.* 1980;142(6):923–933.
18. Gwaltney JM, Sande MA, Austrian R, Hendley JO. Spread of Streptococcus pneumoniae in families. II. Relation of transfer of *S. pneumoniae* to incidence of colds and serum antibody. *J Infect Dis.* 1975;132(1):62–68.
19. McCool TL, Cate TR, Moy G, Weiser JN. The immune response to pneumococcal proteins during experimental human carriage. *J Exp Med*. 2002;195(3):359–365.
20. Zhang Z, Clarke TB, Weiser JN. Cellular effectors mediating Th17-dependent clearance of pneumococcal colonization in mice. *J Clin Invest*. 2009;119(7):1899–1909.
21. Melin M, Jarva H, Siira L, Meri S, Käyhty H, Väkeväinen M. Streptococcus pneumoniae capsular serotype 19F is more resistant to C3 deposition and less sensitive to opsonophagocytosis than serotype 6B. *Infect Immun*. 2009;77(2):676–684.
22. Gordon DL, Johnson GM, Hostetter MK. Ligand-receptor interactions in the phagocytosis of virulent Streptococcus pneumoniae by polymorphonuclear leukocytes. *J Infect Dis.* 1986;154(4):619–626.
23. Kadioglu A, Andrew PW. The innate immune response to pneumococcal lung infection: the untold story. *Trends Immunol.* 2004;25(3):143–149.
24. McCool TL, Weiser JN. Limited role of antibody in clearance of Streptococcus pneumoniae in a murine model of colonization. *Infect Immun.* 2004;72(10):5807–5813.
25. van Rossum AM, Lysenko ES, Weiser JN. Host and bacterial factors contributing to the clearance of colonization by Streptococcus pneumoniae in a murine model. *Infect Immun.* 2005;73(11):7718–7726.
26. Kim JO, Weiser JN. Association of intrastrain phase variation in quantity of capsular polysaccharide and teichoic acid with the virulence of Streptococcus pneumoniae. *J Infect Dis.* 1998;177(2):368–377.
27. Stebbins CE, Galán JE. Structural mimicry in bacterial virulence. *Nature*. 2001;412(6848):701–705.
28. Clark SE, Weiser JN. Microbial modulation of host immunity with the small molecule phosphorylcholine. *Infect Immun*. 2013;81(2):392–401.
29. Fischer W. Phosphocholine of pneumococcal teichoic acids: role in bacterial physiology and pneumococcal infection. *Res Microbiol.* 1999;151(6):421–427.
30. Cundell DR, Gerard NP, Gerard C, Idanpaan-Heikkila I, Tuomanen EI. Streptococcus pneumoniae anchor to activated human cells by the receptor for platelet-activating factor. *Nature*. 1995;377(6548):435–438.
31. Shirasaki H, et al. Expression and localization of platelet-activating factor receptor in human nasal mucosa. *Ann Allergy Asthma Immunol.* 2005;95(2):190–196.
32. Wu H, et al. Lipoxin A4 and platelet activating factor are involved in *E. coli* or LPS-induced lung inflammation in CFTR-deficient mice. *PLoS One.* 2013;9(3):e93003.
33. Hanahan DJ, Demopoulos CA, Liehr J, Pinckard RN. Identification of platelet activating factor isolated from rabbit basophils as acetyl glyceryl ether phosphorylcholine. *J Biol Chem*. 1980;255(12):5514–5516.
34. Clark PO, Hanahan DJ, Pinckard RN. Physical and chemical properties of platelet-activating factor obtained from human neutrophils and monocytes and rabbit neutrophils and basophils. *Biochim Biophys Acta*. 1980;628(1):69–75.
35. Shaw JO, Pinckard RN, Ferrigni KS, McManus LM, Hanahan DJ. Activation of human neutrophils with 1-O-hexadecyl/octadecyl-2-acetyl-sn-glycerol-3-phosphorylcholine (platelet activating factor). *J Immunol.* 1981;127(3):1250–1255.
36. Kitchen E, Rossi AG, Condliffe AM, Haslett C, Chilvers ER. Demonstration of reversible priming of human neutrophils using platelet-activating factor. *Blood*. 1996;88(11):4330–4337.
37. Brown SL, Jala VR, Raghuwanshi SK, Nasser MW, Haribabu B, Richardson RM. Activation and regulation of platelet-activating factor receptor: role of G(i) and G(q) in receptor-mediated chemotactic, cytotoxic, and cross-regulatory signals. *J Immunol.* 2006;177(5):3242–3249.
38. Eckels PC, et al. Amantadine inhibits platelet-activating factor induced clathrin-mediated endocytosis in human neutrophils. *Am J Physiol Cell Physiol.* 2009;297(4):C886–C897.
39. Shalit M, Von Allmen C, Atkins PC, Zweiman B. Platelet activating factor increases expression of complement receptors on human neutrophils. *J Leukoc Biol.* 1988;44(3):212–217.
40. McLaughlin NJ, et al. Platelet-activating factor-mediated endosome formation causes membrane translocation of p67phox and p40phox that requires recruitment and activation of p38 MAPK, Rab5a, and phosphatidylinositol 3-kinase in human neutrophils. *J Immunol.* 2008;180(12):8192–8203.
41. Dalia AB, Weiser JN. Minimization of bacterial size allows for complement evasion and is overcome by the agglutinating effect of antibody. *Cell Host Microbe.* 2011;10(5):486–496.
42. Daley JM, Thomay AA, Connolly MD, Reichner JS, Albina JE. Use of Ly6G-specific monoclonal antibody to deplete neutrophils in mice. *J Leukoc Biol.* 2007;83(1):64–70.
43. Matthias KA, Roche AM, Standish AJ, Shchepetov M, Weiser JN. Neutrophil-toxin interactions promote antigen delivery and mucosal clearance of Streptococcus pneumoniae. *J Immunol.* 2008;180(9):6246–6254.
44. Kinhult J, Egesten A, Benson M, Uddman R, Cardell LO. Increased expression of surface activation markers on neutrophils following migration into the nasal lumen. *Clin Exp Allergy.* 2003;33(8):1141–1146.
45. Kishimoto TK, Jutila MA, Berg EL, Butcher EC. Neutrophil Mac-1 and MEL-14 adhesion proteins inversely regulated by chemotactic factors. *Science.* 1989;245(4923):1238–1241.
46. Tedder TF. Cell-surface receptor shedding: a means of regulating function. *Am J Respir Cell Mol Biol.* 1991;5(4):305–306.
47. Albrich WC, et al. Pneumococcal colonisation density: a new marker for disease severity in HIV-infected adults with pneumonia. *BMJ Open.* 2013;4(8):e005953.
48. Richard AL, Siegel SJ, Erikson J, Weiser JN. TLR2 signaling decreases transmission of Streptococcus pneumoniae by limiting bacterial shedding in an infant mouse Influenza A co-infection model. *PLoS Pathog.* 2014;10(8):e1004339.
49. Hermoso JA, et al. Insights into pneumococcal pathogenesis from the crystal structure of the modular teichoic acid phosphorylcholine esterase

Pce. *Nat Struct Mol Biol.* 2005;12(6):533–538.
50. Zinchuk O, Fukushima A, Zinchuk V, Fukata K, Ueno H. Direct action of platelet activating factor (PAF) induces eosinophil accumulation and enhances expression of PAF receptors in conjunctivitis. *Mol Vis.* 2005;11:114–123.
51. Mori M, Aihara M, Kume K, Hamanoue M, Kohsaka S, Shimizu T. Predominant expression of platelet-activating factor receptor in the rat brain microglia. *J Neurosci.* 1996;16(11):3590–3600.
52. Fernández-Gallardo S, Ortega MP, Priego JG, de Casa-Juana MF, Sunkel C, Sánchez Crespo M. Pharmacological actions of PCA 4248, a new platelet-activating factor receptor antagonist: in vivo studies. *J Pharmacol Exp Ther.* 1990;255(1):34–39.
53. Matsumura Y, Byrne SN, Nghiem DX, Miyahara Y, Ullrich SE. A role for inflammatory mediators in the induction of immunoregulatory B cells. *J Immunol.* 2006;177(7):4810–4817.
54. Garcia CC, et al. Platelet-activating factor receptor plays a role in lung injury and death caused by Influenza A in mice. *PLoS Pathog.* 2009;6(11):e1001171.
55. Dalia AB, Standish AJ, Weiser JN. Three surface exoglycosidases from Streptococcus pneumoniae, NanA, BgaA, and StrH, promote resistance to opsonophagocytic killing by human neutrophils. *Infect Immun.* 2010;78(5):2108–2116.
56. Vollmer W, Tomasz A. Identification of the teichoic acid phosphorylcholine esterase in Streptococcus pneumoniae. *Mol Microbiol.* 2001;39(6):1610–1622.
57. Futosi K, Fodor S, Mócsai A. Reprint of Neutrophil cell surface receptors and their intracellular signal transduction pathways. *Int Immunopharmacol.* 2013;17(4):1185–1197.
58. Krause KH, Schlegel W, Wollheim CB, Andersson T, Waldvogel FA, Lew PD. Chemotactic peptide activation of human neutrophils and HL-60 cells. Pertussis toxin reveals correlation between inositol trisphosphate generation, calcium ion transients, and cellular activation. *J Clin Invest.* 1985;76(4):1348–1354.
59. Santibanez TA, Shefer A, Briere EC, Cohn AC, Groom AV. Effects of a nationwide Hib vaccine shortage on vaccination coverage in the United States. *Vaccine.* 2012;30(5):941–947.
60. Timothy FM, Aimee LB, Andrew TS, Sanjay S. Persistent colonization by Haemophilus influenzae in chronic obstructive pulmonary disease. *Am J Respir Crit Care Med.* 2004;170(3):266–272.
61. Zola TA, Lysenko ES, Weiser JN. Mucosal clearance of capsule-expressing bacteria requires both TLR and nucleotide-binding oligomerization domain 1 signaling. *J Immunol.* 2008;181(11):7909–7916.
62. Fan X, Goldfine H, Lysenko E, Weiser JN. The transfer of choline from the host to the bacterial cell surface requires glpQ in Haemophilus influenzae. *Mol Microbiol.* 2001;41(5):1029–1036.
63. Janson H, Melhus A, Hermansson A, Forsgren A. Protein D, the glycerophosphodiester phosphodiesterase from Haemophilus influenzae with affinity for human immunoglobulin D, influences virulence in a rat otitis model. *Infect Immun.* 1994;62(11):4848–4854.
64. Weiser JN. The pneumococcus: why a commensal misbehaves. *J Mol Med (Berl).* 2010;88(2):97–102.
65. Desa MN, Sekaran SD, Vadivelu J, Parasakthi N. Distribution of CBP genes in Streptococcus pneumoniae isolates in relation to vaccine types, penicillin susceptibility and clinical site. *Epidemiol Infect.* 2008;136(7):940–942.
66. Gosink KK, Mann ER, Guglielmo C, Tuomanen EI, Masure HR. Role of novel choline binding proteins in virulence of Streptococcus pneumoniae. *Infect Immun.* 2000;68(10):5690–5695.
67. Höltje JV, Tomasz A. Teichoic acid phosphorylcholine esterase. A novel enzyme activity in pneumococcus. *J Biol Chem.* 1974;249(21):7032–7034.
68. Paulson SK, Wolf JL, Novotney-Barry A, Cox CP. Pharmacologic characterization of the rabbit neutrophil receptor for platelet-activating factor. *Proc Soc Exp Biol Med.* 1990;195(2):247–254.
69. Stenton SC, et al. Platelet-activating factor in bronchoalveolar lavage fluid from asthmatic subjects. *Eur Respir J.* 1990;3(4):408–413.
70. Yan JJ, et al. Therapeutic effects of lysophosphatidylcholine in experimental sepsis. *Nat Med.* 2004;10(2):161–167.
71. Prescott SM, Zimmerman GA, McIntyre TM. Platelet-activating factor. *J Biol Chem.* 1990;265(29):17381–17384.
72. Siegel SJ, Roche AM, Weiser JN. Influenza promotes pneumococcal growth during coinfection by providing host sialylated substrates as a nutrient source. *Cell Host Microbe.* 2014;16(1):55–67.
73. Weiser JN, Shchepetov M, Chong ST. Decoration of lipopolysaccharide with phosphorylcholine: a phase-variable characteristic of Haemophilus influenzae. *Infect Immun.* 1997;65(3):943–950.
74. Weiser JN, Goldberg JB, Pan N, Wilson L, Virji M. The phosphorylcholine epitope undergoes phase variation on a 43-kilodalton protein in Pseudomonas aeruginosa and on pili of Neisseria meningitidis and Neisseria gonorrhoeae. *Infect Immun.* 1998;66(9):4263–4267.
75. Barbier M, et al. Lysine trimethylation of EF-Tu mimics platelet-activating factor to initiate Pseudomonas aeruginosa pneumonia. *mBio.* 2012;4(3):13.
76. Waller AK, Sage T, Kumar C, Carr T, Gibbins JM, Clarke SR. Staphylococcus aureus lipoteichoic acid inhibits platelet activation and thrombus formation via the Paf receptor. *J Infect Dis.* 2013;208(12):2046–2057.
77. Hosoki K, et al. Staphylococcus aureus directly activates eosinophils via platelet-activating factor receptor. *J Leukoc Biol.* 2012;92(2):333–341.
78. Liu M, et al. Group A Streptococcus secreted esterase hydrolyzes platelet-activating factor to impede neutrophil recruitment and facilitate innate immune evasion. *PLoS Pathog.* 2011;8(4):e1002624.
79. McIntyre TM, Prescott SM, Stafforini DM. The emerging roles of PAF acetylhydrolase. *J Lipid Res.* 2009;50(suppl):S255–S259.
80. Touqui L, et al. Excretion of platelet activating factor-acetylhydrolase and phospholipase A2 into nasal fluids after allergenic challenge: possible role in the regulation of platelet activating factor release. *J Allergy Clin Immunol.* 1994;94(1):109–119.
81. Seki M, et al. Expression and DNA microarray analysis of a platelet activating factor-related molecule in severe pneumonia in mice due to influenza virus and bacterial co-infection. *Jpn J Infect Dis.* 2008;62(1):6–10.
82. Investigators S, et al. Darapladib for preventing ischemic events in stable coronary heart disease. *N Engl J Med.* 2014;370(18):1702–1711.
83. Tettelin H, et al. Complete genome sequence of a virulent isolate of Streptococcus pneumoniae. *Science.* 2001;293(5529):498–506.
84. Clarke TB, Davis KM, Lysenko ES, Zhou AY, Yu Y, Weiser JN. Recognition of peptidoglycan from the microbiota by Nod1 enhances systemic innate immunity. *Nat Med.* 2010;16(2):228–231.
85. Brown AO, et al. Streptococcus pneumoniae translocates into the myocardium and forms unique microlesions that disrupt cardiac function. *PLoS Pathog.* 2014;10(9):e1004383.
86. Radin JN, Orihuela CJ, Murti G, Guglielmo C, Murray PJ, Tuomanen EI. beta-Arrestin 1 participates in platelet-activating factor receptor-mediated endocytosis of Streptococcus pneumoniae. *Infect Immun.* 2005;73(12):7827–7835.
87. Lee W-BB, et al. Neutrophils Promote mycobacterial trehalose dimycolate-induced lung inflammation via the mincle pathway. *PLoS Pathog.* 2011;8(4):e1002614.
88. McGovern NN, et al. Hypoxia selectively inhibits respiratory burst activity and killing of Staphylococcus aureus in human neutrophils. *J Immunol.* 2010;186(1):453–463.
89. Diavatopoulos DA, et al. Influenza A virus facilitates Streptococcus pneumoniae transmission and disease. *FASEB J.* 2010;24(6):1789–1798.
90. Beisswenger C, Lysenko ES, Weiser JN. Early bacterial colonization induces toll-like receptor-dependent transforming growth factor beta signaling in the epithelium. *Infect Immun.* 2009;77(5):2212–2220.
91. Standish AJ, Weiser JN. Human neutrophils kill Streptococcus pneumoniae via serine proteases. *J Immunol.* 2009;183(4):2602–2609.